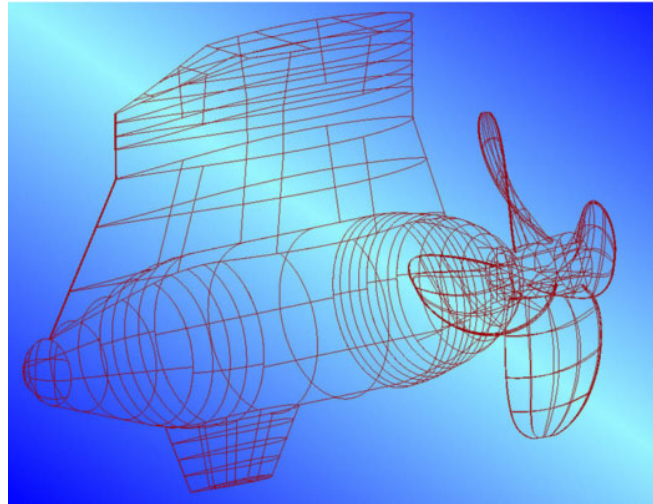


Calculation and Validation of a POD Propulsion System using CFD Codes

F. J. Del Corral (CEHIPAR)
I. Trejo (SEAPLACE)
J. Valle (CEHIPAR)



The new POD propulsion systems are innovative and very used nowadays both in military and commercial ships. Nevertheless CFD (Computational Fluid Dynamics) calculations and validations for these systems are not often found. In this paper the results obtained using a viscous flow CFD code are presented, comparing them with those from model tests. The configuration used for this validation is a single POD with a four blades propeller. Rotary domain is used for the propeller and a fixed domain is used for the POD structure. The goals of the paper are the calculation of a propeller in free water, the calculation of the whole Pod system, including the interaction between the propeller and its structure, and the validation with the results of the model tests done at CEHIPAR.

KEY WORDS

CFD; Validation; Propulsion; Propeller; POD.

INTRODUCTION

The POD azimuthal electrical propulsion systems are still innovative, so there are not many CFD calculations available for this propulsion systems and validation, comparing with experimental results, are almost inexistent.

The POD propulsion systems have one or two propellers directly connected to the shaft of an electrical motor introduced in a casing under the water. All the system, including the electrical motor, the casing and the propellers, can turn 360° around a vertical axis in the stern of the ship. A typical POD solution is shown in Figure 1 and a comparison of the different propulsion systems usually used in ships is shown in Figure 2.

The main benefits of the Diesel-electrical propulsion are:

- Fuel consumption reduction.
- Flexibility for equipment distribution.
- Lower maintenance costs.
- Space reduction.
- Gas emission reduction.

If the Diesel-electrical propulsion is combined with a POD system, the following added benefits are obtained:

- Propulsive power reduction.
- Noise and vibrations reduction.
- Good manoeuvring without transversal propeller in the bow.
- Compact propulsion equipments.
- Costs reduction.
- Hull shape design flexibility.



Fig. 1. POD propulsion system.

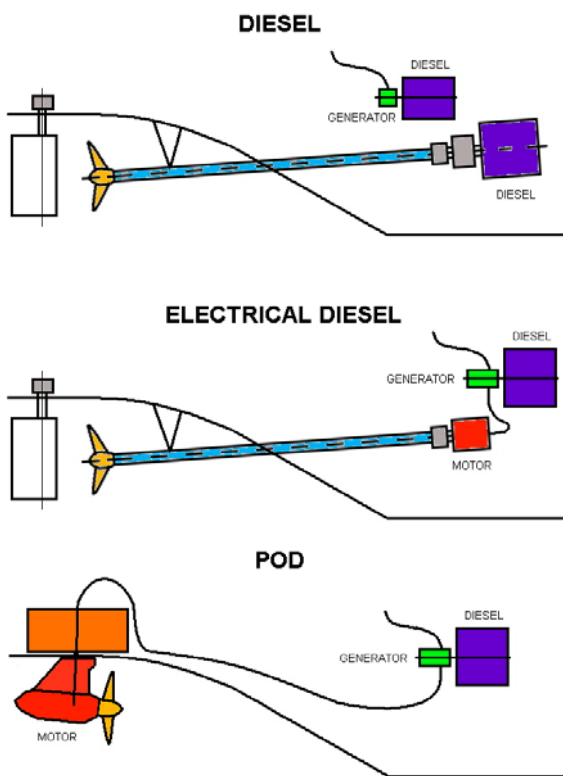


Fig. 2. Propulsion systems comparison.

The main objective of this paper is to validate the calculations, done with a RANSE viscous flow CFD code, of a POD propulsion system performance. The work was made in the following steps:

- CAD Propeller and POD surface definition.
- Conversion of the CAD files to ICEM format.
- Shape cleaning and refining.
- Meshing.
- CFD Calculation.
- Validation of CFD, comparing with experimental results.

All the previous steps were done for a single propeller and for the whole POD propulsion system. The POD system was previously tested at CEHIPAR using their stock propeller E660 (Starboard propeller, 4 blades, 0.17 m diameter, no hub). The POD models installed in a ship model are shown in Figure 3.



Fig. 3. Tested POD system.

The CFD code used for the calculation was the commercial RANSE solver ANSYS CFX[®] with the commercial meshing tool ICEM[®].

CALCULATION METHODOLOGY

As it is well known, the fluid dynamic processes are governed by the Navier-Stokes equations. These equations are a system of second order differential equations that can not be analytically solved for complex systems. So, numerical methods are used to solve the problem by means of Computerized Fluid Dynamics (CFD)

In this paper a RANSE method with finite volumes centred in the vertex has been used. For this finite volume method the computational domain has to be meshed using tetrahedrons, pyramids, prisms or hexahedrons. In this case tetrahedrons and prisms have been used.

For turbulent flow in RANSE calculations, as in this case, it is necessary to use a turbulence model. There are many turbulence models as:

- Eddy Viscosity Turbulence models: In these models the Reynolds Stresses are proportional to the gradient of the velocity. The following turbulence models are in this group:
 - Zero equation: In this case the turbulent eddy viscosity is constant in the entire computational domain. Its field of application is the accelerated flows in nozzles, as air and water jets.
 - K- ϵ model: This is an energy model to be used far from the walls and with moderate viscosity effects.
 - K- ω model: This model is used in the near wall zone and with low Reynolds. It is a good model to compute pressures on surfaces.
 - Shear Stress Transport, SST, model: Developed by Menter it combines the K- ω and K- ϵ models. It is a good method to predict flow separation with adverse gradients of pressure.

- Reynolds Stress models: These models solve the transport equation for the Reynolds Stresses, taking into account the curvature effects in the streamlines and the sudden changes in the stresses. It is used for transitory models, noise simulation and pulsate phenomena. The following turbulence models are in this group:
 - BSL Reynolds Stress.
 - SSG Reynolds Stress.
 - LRR Reynolds Stress.
 - QI Reynolds Stress.
 - ω Reynolds Stress.

The turbulence model used in this paper is the K- ϵ model, which is appropriate to the calculation characteristics.

CALCULATION DETAILS

CAD Surface Definition

The CAD surface definition process is critical to obtain a good mesh definition for the calculations. The main aspects to take into account are:

- Element duplicity.
- Surface unions and intersections.
- Singularities.
- Unit coherency.
- Reference system coherency.
- Smooth surfaces.

In this case, as the code used to generate the mesh was ICEM[®], it was very important to use formats compatible with ICEM[®].

The process started with the definition of the sections of the propeller blades, as a cloud of points generated with the program Helice, developed by CEHIPAR. It is possible to define the sections using systematic series or manually.

The cloud of points was afterwards transformed to smooth surfaces, with tangential continuity in their boundaries. All the process has been done with commercial software as Mastercam[®] and MicroStation[®].

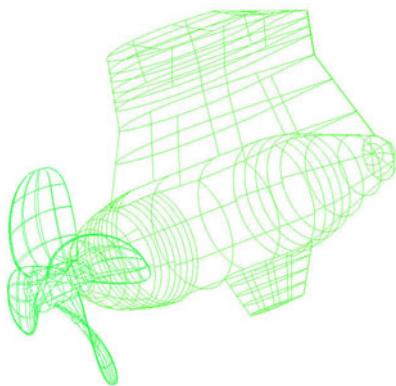


Fig. 4. POD and Propeller Surfaces.

The surfaces were put together to generate a solid using the commercial software SolidWorks[®]. The solid was exported to ICEM[®] using ParaSolid format.

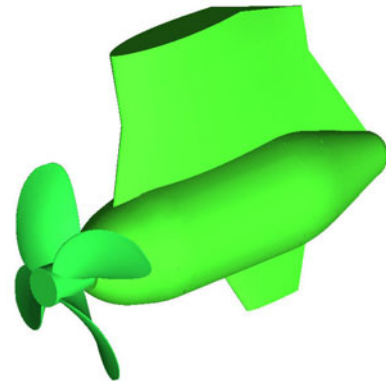


Fig. 5. POD and Propeller Solid.

Computational Domains

The computational domains are the regions in the space used by the CFD program to do the calculations. In the POD calculation there are two types of domains, attending to the movement: stationary and rotational.

In both cases, the propeller and the POD calculations, the computational domain is composed of an external fixed cylindrical domain, simulating the stationary axial flow conditions, and an internal rotational domain, including the propeller that turns with the rotational domain with the angular velocity of the propeller for the computing case.

In both cases the external fixed domain is the same: a cylinder with a radius three times the propeller radius and a length eight times the propeller radius.

The internal rotational domain used to calculate the propeller alone, shown in Figure 6, is a cylinder with a radius one and a half times the propeller radius and a length three times the propeller radius.

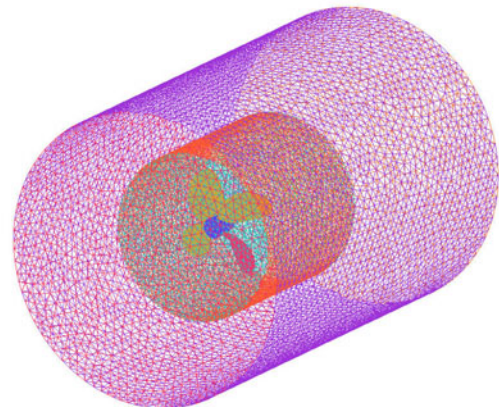


Fig. 6. Computational Domains for Propeller Calculation.

The most important part of this paper is the calculation of the whole POD system. In this case the computational domain used for the propeller can not be used because the casing of the POD will be inside the rotational domain and will turn together with the propeller. To solve this problem a new rotational domain including only the propeller in length was used. This computational domain is shown in Figure 7.

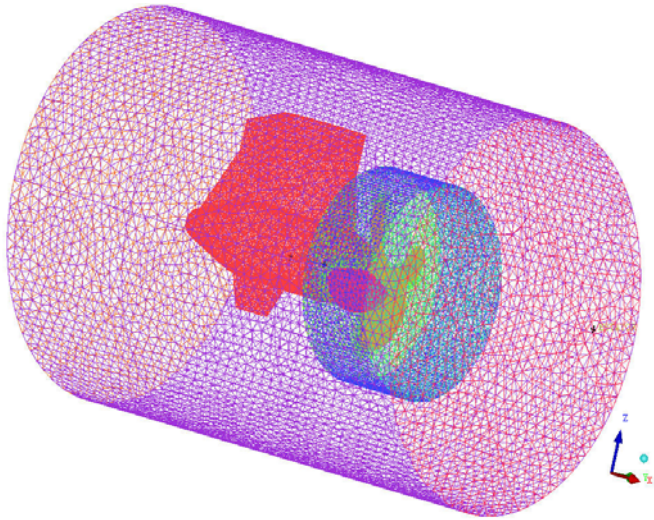


Fig. 7. Computational Domains for POD Calculation.

Meshing

The quality of the mesh is critical in CFD calculation using RANSE methods. In this paper a non-structured mesh of tetrahedrons was used in all cases, including prisms layers in the boundary layer zones.

In order to obtain a better mesh definition in the blades boundaries, a narrow band was added in the border in the geometrical definition of the propeller.

To analyze the influence of the mesh in the results, three different mesh configurations were used for all the computed cases.

Table 1. Mesh Configuration for Propeller Computation.

Mesh	Number of Nodes	Number of Elements
1	434432	1588885
2	1187564	3877590
3	592659	2130019

Table 2: Mesh Configuration for POD Computation.

Mesh	Number of Nodes	Number of Elements
4	310964	1358028
5	584964	2414923
6	369967	1524288

The boundaries of the propeller blades and the POD were analyzed using the tool “Mesh Cut Plane”, in order to detect irregularities or bad mesh configurations in the critical parts. Examples of this kind of analysis are shown in Figures 8 and 9.

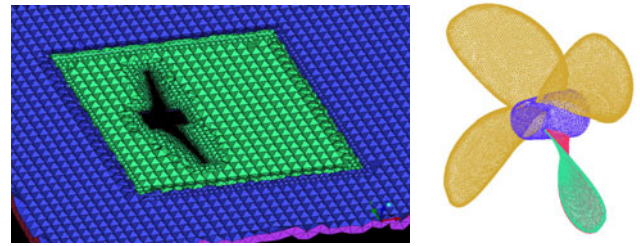


Fig. 8. Mesh Quality Analysis for the Propeller.

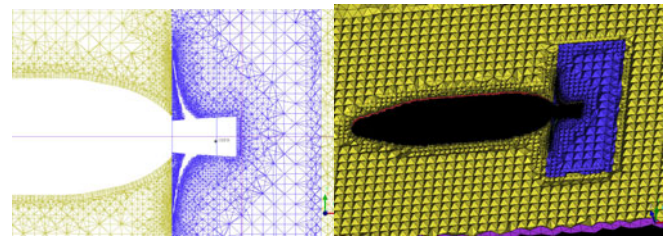


Fig. 9. Mesh Quality Analysis for the POD.

General Characteristics and Boundary Conditions

The fluid used for the calculation was water with the following characteristics:

- Density: 1000 [kg/m³]
- Cinematic Viscosity: 8.899E-4 [Pa s]

The general conditions for the external fixed computational domain were:

- Pressure: 1 atm.
- Buoyancy: Non Buoyant
- Domain Motion: Stationary.
- Heat Transfer Model: None.
- Turbulence Model: k-ε.
- Turbulence Wall Function: Scalable.

The general conditions for the internal rotational computational domain were:

- Pressure: 1 atm.
- Buoyancy: Non Buoyant
- Domain Motion: Rotating: propeller velocity
- Heat Transfer Model: None.
- Turbulence Model: k-ε.
- Turbulence Wall Function: Scalable.

The boundary conditions were:

- Inlet: Axial Velocity.
- Outlet: Average Static Pressure.
- Sides: Free Slip Wall.
- Frame Change: Frozen Rotor.

The used convergence criterion was a R.M.S. lower than 10⁻⁴.

Computed Cases

Four axial velocities were used for the calculation with each mesh, using the same velocities that were used in the models tests to facilitate the validation. A total of 24 cases were computed.

The same revolutions, n , were used for the propeller and the POD, but due to the model test characteristics, different values for the propeller advance ratio J were obtained for both cases, where J is:

$$J = \frac{V}{nD} \quad (1)$$

The computed cases are resumed in Tables 3 and 4.

Table 3. Computed Cases for Propeller Computation with $n=21.952$ rps.

V (m/s)	J
1.395	0.3738
2.198	0.5890
2.990	0.8012
4.386	1.1753

Table 4. Computed Cases for POD Computation with $n=23.454$ rps.

V (m/s)	J
1.395	0.3499
2.198	0.5513
2.990	0.7499
4.386	1.1000

RESULTS

The results obtained for thrust, torque and efficiency of the propeller, with and without the POD, for all the computed velocities will be presented in this section. Normally these data are presented in non-dimensional format, using the thrust, torque and efficiency coefficients, K_T , K_Q and η_0 in Equations (1), (2) and (3). The differences with the experimental data are presented as percentages of error.

$$K_T = \frac{T}{\rho n^2 D^4} \quad (2)$$

$$K_Q = \frac{Q}{\rho n^2 D^5} \quad (3)$$

$$\eta_0 = \frac{J}{2\pi} \frac{K_T}{K_Q} \quad (4)$$

In this paper the results for the propeller alone will be presented first and then the results for the whole POD system.

The validation will be done using the percentage of error and the increment of the magnitudes referred to the experimental data, because when the thrust and torque values are low the percentage of error is high but the increment is low and the conclusions of the study would be distorted.

Experimental Data Results

Table 5. Non-Dimensional Results for Propeller. Experimental Data.

J	K_T	$100 \cdot K_Q$	η_0
0.3738	0.4115	7.0766	0.35
0.5890	0.3192	5.7621	0.52
0.8012	0.2234	4.3690	0.65
1.1753	0.0510	1.5501	0.61

Table 6. Dimensional Results for Propeller. Experimental Data.

V (m/s)	T (kg)	Q (kg·cm)
1.395	16.8827	49.3596
2.198	13.0961	40.1907
2.990	9.1670	30.4740
4.386	2.0906	10.8120

Table 7. Non-Dimensional Results for POD. Experimental Data.

J	K_T	$100 \cdot K_Q$	η_0
0.3499	0.4424	7.4968	0.33
0.5513	0.3622	6.3404	0.50
0.7499	0.2764	5.1369	0.64
1.1000	0.1254	2.8358	0.77

Table 8. Dimensional Results for POD. Experimental Data.

V (m/s)	T (kg)	Q (kg·cm)
1.395	20.7182	59.6892
2.198	16.9650	50.4820
2.990	12.9470	40.9000
4.386	5.8710	22.5790

Calculation Data Results

Propeller Thrust

Table 9. Mesh 1. Non-Dimensional Results for Propeller Thrust.

J	K_T	Error K_T (%)
0.3738	0.4026	2.1568
0.5890	0.3214	0.6808
0.8012	0.2293	2.6192
1.1753	0.0472	7.3010

Table 10. Mesh 2. Non-Dimensional Results for Propeller Thrust.

J	K_T	$Error K_T (%)$
0.3738	0.4022	2.2491
0.5890	0.3160	0.9902
0.8012	0.2220	0.6446
1.1753	0.0410	19.5914

Table 11. Mesh 3. Non-Dimensional Results for Propeller Thrust.

J	K_T	$Error K_T (%)$
0.3738	0.4058	1.3738
0.5890	0.3237	1.4277
0.8012	0.2295	2.7044
1.1753	0.0392	23.1235

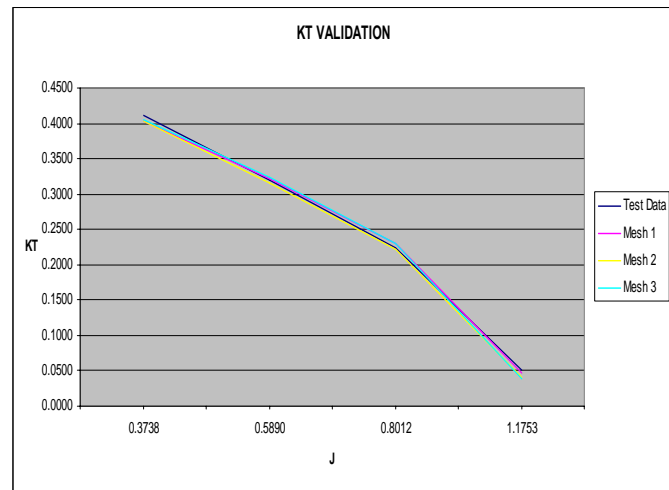


Fig. 10. Propeller. K_T Validation.

Table 12. Mesh 1. Results for Propeller Thrust Increments.

V (m/s)	T (kg)	ΔT (kg)
1.395	16.5185	0.3641
2.198	13.1853	0.0892
2.990	9.4071	0.2401
4.386	1.9380	0.1526

Table 13. Mesh 2. Results for Propeller Thrust Increments.

V (m/s)	T (kg)	ΔT (kg)
1.395	16.5029	0.3797
2.198	12.9664	0.1297
2.990	9.1079	0.0591
4.386	1.6810	0.4096

Table 14. Mesh 3. Results for Propeller Thrust Increments.

V (m/s)	T (kg)	ΔT (kg)
1.395	16.6507	0.2319
2.198	13.2831	0.1870
2.990	9.4149	0.2479
4.386	1.6072	0.4834

POD Thrust

Table 15. Mesh 4. Non-Dimensional Results for POD Thrust.

J	K_T	$Error K_T (%)$
0.3499	0.4404	0.4426
0.5513	0.3746	3.4097
0.7499	0.2925	5.8156
1.1000	0.1534	22.3923

Table 16. Mesh 5. Non-Dimensional Results for POD Thrust.

J	K_T	$Error K_T (%)$
0.3499	0.4318	2.3915
0.5513	0.3611	0.3223
0.7499	0.2917	5.5275
1.1000	0.1513	20.6591

Table 17. Mesh 6. Non-Dimensional Results for POD Thrust.

J	K_T	$Error K_T (%)$
0.3499	0.4303	2.7313
0.5513	0.3669	1.3030
0.7499	0.2958	7.0150
1.1000	0.1532	22.1736

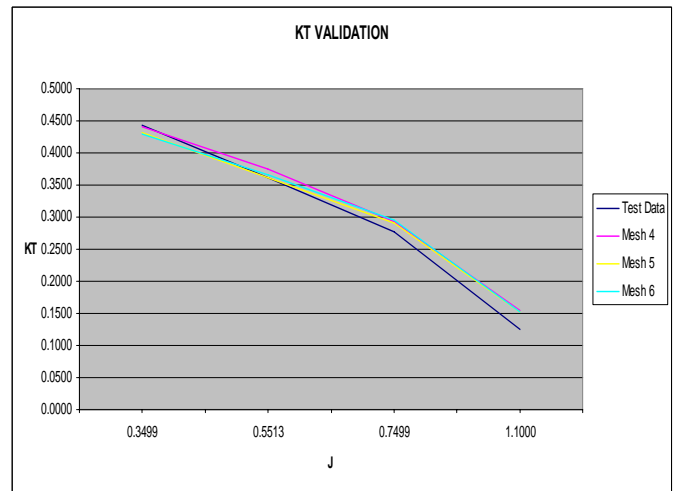


Fig. 11. POD. K_T Validation.

Table 18. Mesh 4. Results for Propeller Thrust Increments.

V (m/s)	T (kg)	ΔT (kg)
1.395	20.6265	0.0917
2.198	17.5435	0.5785
2.990	13.6999	0.7529
4.386	7.1857	1.3147

Table 19. Mesh 5. Results for Propeller Thrust Increments.

V (m/s)	T (kg)	ΔT (kg)
1.395	20.2227	0.4955
2.198	16.9103	0.0547
2.990	13.6626	0.7156
4.386	7.0839	1.2129

Table 20. Mesh 6. Results for Propeller Thrust Increments.

V (m/s)	T (kg)	ΔT (kg)
1.395	20.1523	0.5659
2.198	17.1861	0.2211
2.990	13.8552	0.9082
4.386	7.1728	1.3018

In the previous data there are errors greater than 20% when the velocities are high, but the increments are lower than 500 grams for the propeller and 1 kg for the POD.

Propeller Torque

Table 21. Mesh 1. Non-Dimensional Results for Propeller Torque.

J	$100 \cdot K_Q$	$Error K_Q$ (%)
0.3738	7.0578	0.2666
0.5890	5.9329	2.9635
0.8012	4.6548	6.5416
1.1753	1.9026	22.7415

Table 22. Mesh 2. Non-Dimensional Results for Propeller Torque.

J	$100 \cdot K_Q$	$Error K_Q$ (%)
0.3738	7.0438	0.4639
0.5890	5.7334	0.4988
0.8012	4.4366	1.5473
1.1753	1.6680	7.6053

Table 23. Mesh 3. Non-Dimensional Results for Propeller Torque.

J	$100 \cdot K_Q$	$Error K_Q$ (%)
0.3738	7.1000	0.3298
0.5890	5.9597	3.4299
0.8012	4.6421	6.2509
1.1753	1.7064	10.0848

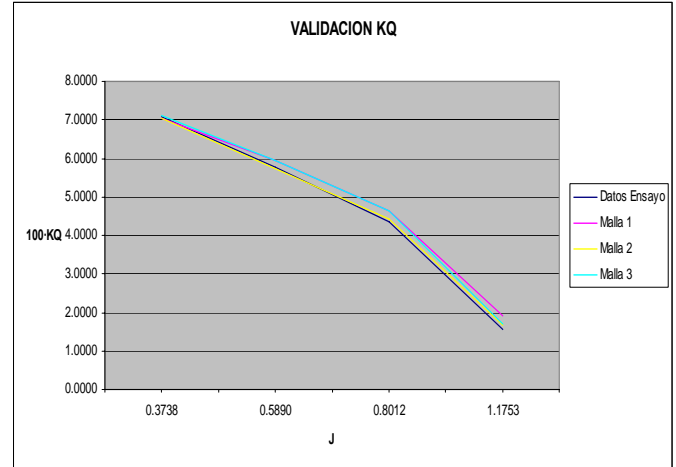


Fig. 12. Propeller. K_Q Validation.

Table 24. Mesh 1. Results for Propeller Torque Increments.

V (m/s)	Q (kg-cm)	ΔQ (kg-cm)
1.395	49.2280	0.1316
2.198	41.3817	1.1910
2.990	32.4675	1.9935
4.386	13.2708	2.4588

Table 25. Mesh 2. Results for Propeller Torque Increments.

V (m/s)	Q (kg-cm)	ΔQ (kg-cm)
1.395	49.1306	0.2290
2.198	39.9902	0.2005
2.990	30.9455	0.4715
4.386	11.6343	0.8223

Table 26. Mesh 3. Results for Propeller Torque Increments.

V (m/s)	Q (kg-cm)	ΔQ (kg-cm)
1.395	49.5224	0.1628
2.198	41.5692	1.3785
2.990	32.3789	1.9049
4.386	11.9024	1.0904

POD Torque

Table 27. Mesh 4. Non-Dimensional Results for POD Torque.

J	$100 \cdot K_Q$	$Error K_Q (\%)$
0.3499	7.3786	1.5763
0.5513	6.5293	2.9798
0.7499	5.6516	10.0196
1.1000	3.6146	27.4597

Table 28. Mesh 5. Non-Dimensional Results for POD Torque.

J	$100 \cdot K_Q$	$Error K_Q (\%)$
0.3499	7.3915	1.4046
0.5513	6.2747	1.0351
0.7499	5.4511	6.1174
1.1000	3.6361	28.2201

Table 29. Mesh 6. Non-Dimensional Results for POD Torque.

J	$100 \cdot K_Q$	$Error K_Q (\%)$
0.3499	7.2763	2.9410
0.5513	6.3747	0.5414
0.7499	5.5216	7.4895
1.1000	3.6277	27.9248

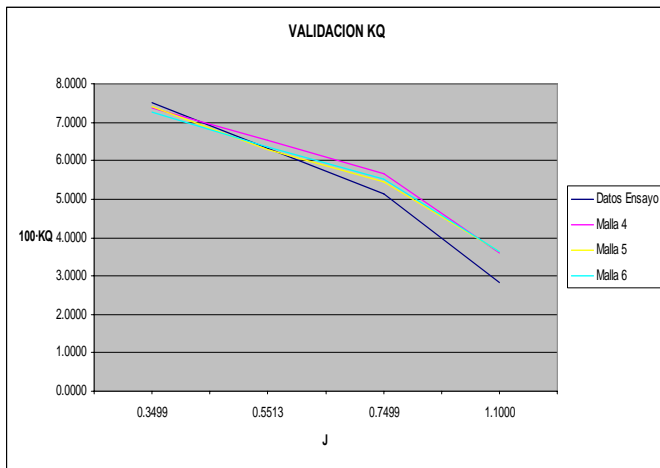


Fig. 13. POD. K_Q Validation.

Table 30. Mesh 4. Results for POD Torque Increments.

V (m/s)	Q (kg-cm)	ΔQ (kg-cm)
1.395	58.7483	0.9409
2.198	51.9863	1.5043
2.990	44.9980	4.0980
4.386	28.7791	6.2001

Table 31. Mesh 5. Results for POD Torque Increments.

V (m/s)	Q (kg-cm)	ΔQ (kg-cm)
1.395	58.8508	0.8384
2.198	49.9595	0.5225
2.990	43.4020	2.5020
4.386	28.9508	6.3718

Table 32. Mesh 6. Results for POD Torque Increments.

V (m/s)	Q (kg-cm)	ΔQ (kg-cm)
1.395	57.9337	1.7555
2.198	50.7553	0.2733
2.990	43.9632	3.0632
4.386	28.8841	6.3051

In this case the differences of the absolute values are higher than in the thrust but the increments presentation is also useful.

Propeller Efficiency

Table 33. Mesh 1. Results for Propeller Efficiency.

J	η_0	$Error \eta_0 (\%)$
0.3738	0.34	1.8953
0.5890	0.51	2.2170
0.8012	0.63	3.6816
1.1753	0.46	24.4763

Table 34. Mesh 2. Results for Propeller Efficiency.

J	η_0	$Error \eta_0 (\%)$
0.3738	0.34	1.7935
0.5890	0.52	0.4939
0.8012	0.64	2.1584
1.1753	0.46	25.2745

Table 35. Mesh 3. Results for Propeller Efficiency.

J	η_0	$Error \eta_0 (\%)$
0.3738	0.34	1.6980
0.5890	0.51	1.9357
0.8012	0.63	3.3379
1.1753	0.43	30.1661

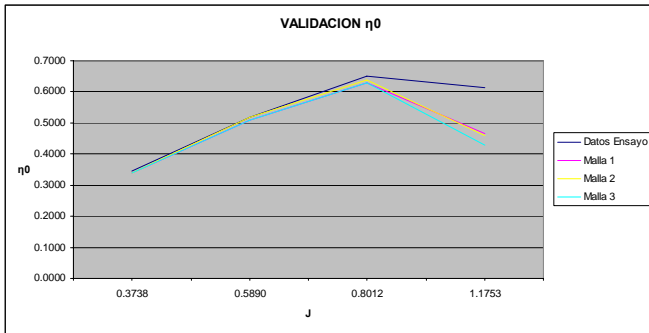


Fig. 14. Propeller. η_0 Validation.

Convergency

The convergence of the calculation method is better for the whole POD system than for the propeller alone. This can be explained because the POD casing smoothes and homogenises the streamlines.

A relation between the mesh number of elements and the number of iterations necessary to achieve the convergence has not been observed.

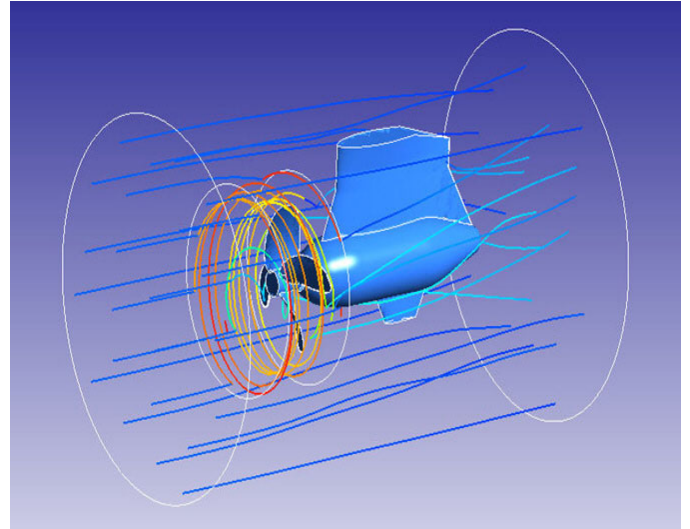


Fig. 16. POD streamlines.

POD Efficiency

Table 36. Mesh 4. Results for POD Efficiency.

J	η_0	Error η_0 (%)
0.3499	0.33	1.1519
0.5513	0.50	0.4175
0.7499	0.62	3.8211
1.1000	0.74	3.9757

Table 37. Mesh 5. Results for POD Efficiency.

J	η_0	Error η_0 (%)
0.3499	0.33	1.0009
0.5513	0.50	0.7203
0.7499	0.64	0.5559
1.1000	0.73	5.8969

Table 38. Mesh 6. Results for POD Efficiency.

J	η_0	Error η_0 (%)
0.3499	0.33	0.2161
0.5513	0.51	0.7575
0.7499	0.64	0.4414
1.1000	0.74	4.4958

CONCLUSIONS

- For low velocities, the results obtained for all the velocities for the propeller and the POD are very similar to the experimental results.
- It is very useful to present the results for the validation as magnitudes increments, as well as percentages of error.
- The calculated values are similar for the three studied meshes for all the velocities, but are better for lower than for higher velocities.
- The analysis of the validity of different turbulence models depending on the axial velocity will be an interesting future work.
- For all the velocities, for both Propeller and POD, it has not been observed a direct relation between the results and the number of elements used in the mesh.
- CFD tools are applicable for the analysis of propellers and POD, especially for low velocities.
- The convergence of the calculation method is better for the whole POD system than for the propeller alone.
- A relation between the mesh number of elements and the number of iterations necessary to achieve the convergence has not been observed.

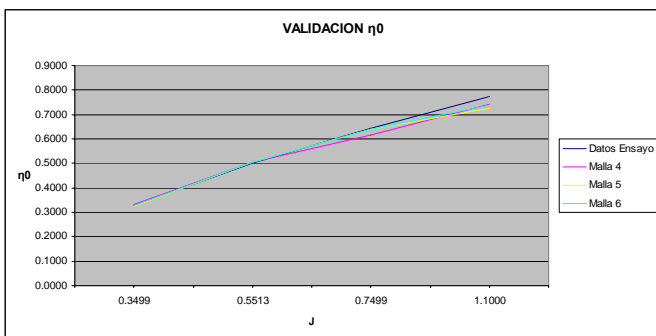


Fig. 15. POD. η_0 Validation.

REFERENCES

ANSYS CFX-11. Documentation.

Trejo I., Terceño M., Valle J., Iranzo A. y Domingo J.
– Analysis of a ship propeller using CFD codes –
International Conference on Computational Methods
in Marine Engineering, MARINE 2007.

Brizzolara S., VillaD. Y Gaggero S. – A systematic
comparison between RANS and Panel methods for
propeller análisis.

Haimov H., Terceño M. y Trejo I. – Use of commercial
RANSE code for open water propeller calculations –
10th NUTTS, Hamburg 2007.

Stuart Jessup – Experimental Data for RANS
Calculations and Comparisons (DTMB 4119) -
Procedures of 22nd ITTC Propulsion Committee
Propeller RANS, Panel Method Workshop, 1998.